

T-Matrix Formulation of Impurity Scattering in Correlated Systems

W. Ziegler, D. Poilblanc*, R. Preuss, W. Hanke and D. J. Scalapino[†]

*Institut für Theoretische Physik, Universität Würzburg
97074 Würzburg, FRG.*

**Laboratoire de Physique Quantique, Université Paul Sabatier,
31062 Toulouse, France.*

*[†] Department of Physics, University of California at Santa Barbara,
Santa Barbara, California 93106.*

Using a generalized T-matrix description which, in principle, exactly includes Coulomb correlations and potential scattering events, resonant and bound impurity states are discussed. Like in the non-interacting case, the effects of the scattering potential can be divided into different partial wave channels, exploiting the symmetry of the underlying lattice. Due to Coulomb correlations bare local (i.e. s-wave) potentials become dynamic and extended, being responsible also for p-, d-wave etc. scattering effects. Numerically exact results for both the two-dimensional t-J and Hubbard models are used to construct a simple (static) approximation to the effective impurity potential which is shown to reproduce the exact resonant scattering and bound states in the relevant symmetry channels.

Experimental data on high- T_c materials including substitutional defects serve for probing their unusual normal state properties as well as the nature of the superconducting phase. Introducing, for example, Zn in the copper oxide planes influences transport and magnetic properties and leads to a drastic reduction of the transition temperature T_c ¹⁻³. The physical conclusions drawn from the results are still controversial. For example, this is the case for the local magnetic moment induced by a non-magnetic impurity such as Zn in hole doped superconducting samples^{1,4-7} which could lead to a magnetic pair breaking mechanism^{8,9}.

However, one *common* feature seems to be the spatially extended nature of the magnetic effects on the CuO-based high- T_c compounds. From residual resistivity measurements one deduces large scattering cross sections of several lattice constants in diameter^{2,3} favoring strong potential scattering likely connected to d-wave pair breaking⁸. On the theoretical side there has been work based on s-wave impurity scattering in anisotropic superconductors revealing the strong influence of non-magnetic impurities¹⁰⁻¹⁴. In addition, calculations were carried out for d-wave superconductors with combined scattering by impurities and Coulomb correlations^{15,16}.

In this paper we focus on the interplay between strong correlations and local potential scattering. This situation can be ascribed to Zn²⁺ impurities with a filled (3d)¹⁰ shell in the cuprate superconductors. We derive a microscopic picture of the mediated scattering processes using a generalized T-matrix description which exactly includes Coulomb correlations and which exploits the symmetries of the underlying lattice. Partial-wave phase shifts are introduced which, like in the non-interacting case determine the additional density of states caused by the impurity potential. For this purpose we take advantage of numerical exact results of translational-invariant lattices and combine them in analytical T-matrix expressions for a single impurity. By doing this we can determine the

effective potential strengths acting in a perturbed t -J system investigated earlier¹⁷.

Consider a correlated two-dimensional system such as the one band Hubbard model with Hamiltonian,

$$H = H_0 + H_U = -t \sum_{\langle i,j \rangle} c_{i\sigma}^\dagger c_{j\sigma} + U \sum_i n_{i\uparrow} n_{i\downarrow}, \quad (1)$$

using standard notations, and a bare impurity operator

$$V_{Imp,\sigma} = \sum_{\delta\sigma} (t_{0\sigma} c_{0\sigma}^\dagger c_{\delta\sigma} + h.c.) + \sum_{\sigma} V_{0\sigma}^{bare} n_{0\sigma}. \quad (2)$$

Here the four bonds connected to the impurity site at the origin are modified by $t_{0\sigma}$. The simplest description of a vacancy is then obtained by setting $t_{0\sigma} = t$. For the sake of simplicity the potential is restricted here to the central site but the following analysis is more general and valid for extended one-body potentials. The above scattering problem on a lattice is defined spin-dependent and can therefore be adapted to different physical scenarios. In the case of non-interacting systems, e.g. $U = 0$, successive scattering is described by the Greens function $G_\sigma = G_0 + G_0 T_\sigma G_0$. Here, the T-matrix, defined as in usual scattering theory, $T_\sigma = V_{Imp,\sigma} (1 - G_0 V_{Imp,\sigma})^{-1}$, involves only the unperturbed propagator G_0 and the bare potential $V_{Imp,\sigma}$.

On the other hand, for correlated systems it is *ad hoc* not clear how to define a T-matrix leading to a similar result for the exact Greens function G . This can be achieved by investigating the representation of G extracted from perturbation theory. For finite temperatures, the exact Greens Function G can be written in the Matsubara formalism and in momentum space as

$$G_\sigma^{-1}(\mathbf{k}, \mathbf{k}', \omega_n) = i\omega_n - \varepsilon(\mathbf{k}) - \Sigma_\sigma(\mathbf{k}, \mathbf{k}', \omega_n). \quad (3)$$

The self-energy Σ is a sum of three terms $\Sigma_U(\mathbf{k}, \mathbf{k}, \omega_n)$, $\Sigma_{UV,\sigma}(\mathbf{k}, \mathbf{k}', \omega_n)$ and $V_{Imp,\sigma}(\mathbf{k}, \mathbf{k}')$. In a diagrammatic

analysis $\Sigma_U(\mathbf{k}, \mathbf{k}, \omega_n)$ contains exclusively many-body effects, the mixed self-energy term $\Sigma_{UV,\sigma}(\mathbf{k}, \mathbf{k}', \omega_n)$ includes all correlation diagrams with an internal line scattered at least once by $V_{Imp,\sigma}$ ¹⁸, examples of which are given in Figs. 1b) and 1c). $V_{Imp,\sigma}(\mathbf{k}, \mathbf{k}')$ is then just a single scattering event caused by the bare impurity potential. Defining a dynamical effective potential

$$V_{eff,\sigma}(\mathbf{k}, \mathbf{k}', \omega_n) = \Sigma_{UV,\sigma}(\mathbf{k}, \mathbf{k}', \omega_n) + V_{Imp,\sigma}(\mathbf{k}, \mathbf{k}') \quad (4)$$

one arrives at the desired formulation, i.e.

$$G_\sigma(\mathbf{k}, \mathbf{k}', \omega_n) = G_U(\mathbf{k}, \mathbf{k}, \omega_n) + G_U(\mathbf{k}, \mathbf{k}, \omega_n) T_\sigma(\mathbf{k}, \mathbf{k}', \omega_n) G_U(\mathbf{k}', \mathbf{k}', \omega_n), \quad (5)$$

where $G_U^{-1}(\mathbf{k}, \mathbf{k}, \omega_n) = i\omega_n - \varepsilon(\mathbf{k}) - \Sigma_U(\mathbf{k}, \mathbf{k}, \omega_n)$ and, by omitting the momentum indices,

$$T_\sigma(\omega_n) = V_{eff,\sigma}(\omega_n) (1 - G_U(\omega_n) V_{eff,\sigma}(\omega_n))^{-1}. \quad (6)$$

In order to investigate the one-particle behavior of the system by means of the T-matrix, one exploits the transformation of its matrix elements in real space according to the symmetrized states of the underlying point-group symmetry of the lattice¹⁹. This means that the effects of the scattering potential, which respects this symmetry, can be divided into contributions to different partial-wave channels. Note that for the non-interacting case, the bare potentials $V_{0\sigma}^{bare}$ and $t_{0\sigma}$ only contribute to s-wave processes, while scattering in the d-, p-wave etc. channels would require extended bare potentials. As seen later, this is substantially modified by the Coulomb interaction leading to correlation induced longer-ranged effective potentials. The poles of the retarded T-matrix, which correspond to the zero-values of its determinant, either determine resonant states, which are found inside the bands of the unperturbed ($V_{Imp} = 0$) system, or bound states separated from the continuum. These statements are clear for non-interacting systems¹⁹ but hold also for $U \neq 0$. Note that $V_{eff,\sigma}(\omega)$ is a real quantity at the bound state energies $\omega = \omega_{BS}$ due to the infinite lifetime of these states.

By using the irreducible representations the complex determinant of the T-matrix factorizes into the subdeterminants of its partial-wave decompositions. The partial-wave phase shifts $\phi_\alpha(\omega)$ are then introduced as the (negative) phase of these α -wave subdeterminants. They determine the additional density of states (DOS) caused by an extended impurity potential¹⁹. The total DOS of the system is given by the trace over the retarded Greens function G^{ret} and can be written as the sum of $D_U(\omega)$, the DOS of the correlated system without the impurity and an additional impurity-caused contribution $\Delta D_\sigma(\omega)$. Bringing in the phase shifts, this leads to

$$\begin{aligned} \Delta D_\sigma(\omega) &= -\frac{1}{N\pi} \text{Im} \frac{\partial}{\partial \omega} \ln \text{Det}(1 - G_U^{ret}(\omega) V_{eff,\sigma}(\omega)), \\ &= \sum_\alpha \Delta D_{\alpha,\sigma}(\omega) = \frac{1}{N\pi} \sum_\nu g(\alpha) \frac{\partial \phi_{\alpha,\sigma}}{\partial \omega}, \end{aligned} \quad (7)$$

where N counts the number of sites and $g(\alpha)$ denotes the degeneracy of the representation α .

This shows that the phase shifts and the T-matrix defined for non-interacting systems are still helpful concepts for studying bound states and resonant scattering in the interacting case. However, the use of Eq.(6) implies the knowledge of the *effective* potential which is *a priori* frequency and interaction (U) dependent. Note that V_{eff} can be expressed as $V_{eff,\sigma}(\omega) = G_U^{ret}(\omega)^{-1} - G_\sigma^{ret}(\omega)^{-1}$, which, in principle, would make it possible to extract the dynamical potentials by numerical calculations. Here we adopt a somewhat simpler approach by showing that a crude static but nevertheless interaction-dependent Ansatz can be made for $V_{eff,\sigma}$ which can describe, within reasonable accuracy, the scattering processes. This method enables us to understand in more physical terms the interplay between the interaction and short-range impurity scattering.

One important feature which has to be included in the Ansatz is the *longer range character* of V_{eff} due to the background of the correlated host. This can simply be seen from the connection between the bare and the dynamically modified potential. By explicitly transforming the Coulomb term to the real-space irreducible representation, one finds local interactions between different wave-symmetries, i.e.

$$H_U = \sum_{\nu, \alpha_1, \alpha_2, \alpha_3, \alpha_4} U_\nu^{\alpha_1 \alpha_2 \alpha_3 \alpha_4} c_{\nu\uparrow}^{\alpha_1\dagger} c_{\nu\uparrow}^{\alpha_2} c_{\nu\downarrow}^{\alpha_3\dagger} c_{\nu\downarrow}^{\alpha_4} \quad (8)$$

where $c_{\sigma\nu}^{(\dagger)}$ are the symmetrized annihilation (creation) operators of the one-particle spin (σ) states. α labels in general all irreducible representations of the site-type ν ²⁰. Note that, although it contains α -wave operators the above expression for H_U is invariant under all the point group symmetries. This implies selection rules on the matrix elements $U_\nu^{\alpha_1 \alpha_2 \alpha_3 \alpha_4}$ which, for simplicity, are not specified here. Therefore, even for a pure s-wave potential $V_0^{bare} \sum_\sigma c_{\sigma 0}^\dagger c_{\sigma 0}^s$ at the origin, incoming d-wave propagators are scattered at $\nu = 1$ from a potential mediated by the Coulomb repulsion as shown in Fig. 1.

This demonstrates that, due to many-body effects, even local (s-wave) potentials always become dynamically *extended*, being in general responsible for scattering contributions in all symmetry channels. In our numerical results the effective potential in Eq.(4) is described by assuming the following static approximation for the effective potential in Eq.(4);

$$V_{eff}^{stat} = t' \sum_\sigma (c_{0\sigma}^\dagger c_{1\sigma}^s + h.c.) + \sum_{\nu\alpha\sigma} V_{\nu\sigma}^\alpha c_{\nu\sigma}^{\alpha\dagger} c_{\nu\sigma}^\alpha. \quad (9)$$

Generally, the ν -off-diagonal (diagonal) part of V_{eff} also takes into account the effective change of the hopping amplitudes (potential terms).

Next, we proceed with our numerical results. At zero

temperature, the retarded Greens function G_U appearing in the above equations is calculated by exact diagonalization (ED) techniques for the half-filled 2D t - J model²¹. In this context, we regard this model¹⁷ as the strong-coupling limit of our original Hamiltonian Eq.(1) to perform the T-matrix calculations (i.e. $J = 4t^2/U$). We consider the situation of reference¹⁷, where an inert site in a t - J lattice produced bound states of different wave symmetries α in the singlet one-particle excitation spectrum. The above formalism is used to determine the effective potential strengths causing these bound states. The description in terms of spin-dependent (effective) potentials takes into account that an excess-spin lifts the spin-degeneracy of the system, leading also to an antiferromagnetic structure in the vicinity of the impurity^{17,22}. In contrast, an infinitesimal magnetic coupling of the inert site to the lattice restores the spin-degeneracy²³, which would lead again to spin-independent effective potentials. Keeping in mind, that we restrict our calculations to the low-lying excitations in the above mentioned singlet channel¹⁷, we omit spin indices from now on. For the case of interest here ($t_0 = t$ or more generally for $V_0^{bare} = 0$) the problem becomes particle-hole symmetric. Then, for simplicity, we define $\omega = 0$ as the lower edge of the quasiparticle band of the t - J -model (lower Hubbard band). In the *hole* representation, positive (negative) values of $V_{0,1,2}^\alpha$ correspond to repulsive (attractive) potentials.

According to the local DOS results of Ref.¹⁷, the values of V_0^α and V_2^α are set to large values $\sim 20t$ in order to expel particles from the corresponding site-types $\nu = 0, 2$. In our calculations t' increases the bound-state energy quadratically. Taking the actual small binding energies of¹⁷ into account the small parameter t' is therefore set to zero. In this sense the derived potential strengths represent an upper limit.

Fig. 2 displays the exact bound state energies ω_{BS} , calculated from the local DOS for a 20-site cluster with an isolated site at the origin¹⁷. By using the T-matrix, the energetic locations of the bound states are reproduced for values of $J = 0.5$ and $J = 1.0$ fixing the effective potentials V_1^α . Fig. 2 also exhibits the dependence of V_1^α on the exchange coupling J of the unperturbed system. As one expects, the attractive potentials increase with J . One finds the actual value of the effective potential to be of the order of J , which is the loss of magnetic energy per bond of the inert site.

Due to the dynamic renormalization, the potential V_1^α acts, as mentioned, differently in each symmetry sector being largest for the s -wave channel. Note that in the limit of vanishing interaction strength ($U \rightarrow 0$), the p - and d -wave potentials also have to vanish, reflecting non-extended potential scattering. Therefore, in an interacting system, there should exist an optimum correlation strength producing the largest effective potentials for bound states.

For $J = 0.5$ Fig. 3a) shows the DOS of the unperturbed

26-site cluster used to calculate the additional impurity-induced density in Fig. 3b). Assuming the effective potentials to be slowly varying functions of ω one finds a suppression of density for small energies in agreement with the exact result¹⁷ in Fig. 3c).

Now, we investigate scattering in the 2D Hubbard model. For finite temperatures, we exploit results of Quantum Monte Carlo (QMC)/Maximum Entropy calculations²⁴ for the undoped system by inserting the unperturbed Greens functions into the T-matrix equations.

At half-filling and for $U = 8t$, $\beta t = 10$, we use the effective potentials derived from the t - J -model for $J = 4t^2/U = 0.5$ and for the particle-hole symmetric case $t_0 = t$. In this case, V_0^{bare} is irrelevant and can be set to zero, while the effective potentials change sign at the chemical potential μ . Both pure systems are characterized by long-range antiferromagnetic correlations being disrupted by the impurity which should lead to a similar behavior regarding the formation of bound states. Actually, the states appearing below the t - J quasiparticle band are now located just above the small dispersive quasiparticle band of width $\sim 2J$ riding on top of a several t wide incoherent background²⁴. This can be seen in Fig. 4 displaying the unperturbed DOS D_U obtained from QMC calculations and the (non-normalized) additional density ΔD_α . Differing from the t - J -case the s -wave contributions are shifted towards the quasiparticle band. The appearance of these states results in an overall effect of narrowing the gap of the unperturbed Hubbard model by almost 20%.

In summary, we have considered a formally exact T-matrix method adapted to correlated systems which revealed the many-body interactions as the origin of dynamically extended potentials. Using numerical data for the unperturbed propagators, we reproduced the static effective potentials causing bound states in a 2D t - J -lattice with an inert site. Applying the formalism to the insulating 2D Hubbard model, we have shown the correspondence of the two models regarding the appearance of spectral weight in the correlation gap. Our result is relevant for T-matrix approximations in the dilute impurity limit, i.e. where the single impurity scattering has to be treated exactly. There, higher symmetry channels than the usually considered s -wave contributions have to be taken into account for interacting systems. Our static, effective potentials in Eq.(9) can, for example, directly be used as an input to a cluster diagonalization approach, where the effect of potential impurity scattering in a 2D superconductor described by a BCS mean-field theory²⁵ is studied. In ref.²⁵ the impurity potential was parameterized. Nevertheless, already this work demonstrated that the range of the impurity potential is of quantitative importance in the case of strong potential scatterers.

D. P. and W. H. acknowledge hospitality and support

from the Physics Department Santa Barbara. The QMC calculations were performed at HLRZ Jülich and at LRZ München. D. P. also thanks IDRIS (Orsay) for providing CPU time for the ED calculations.

-
- ¹ G. Xiao *et al.*, Phys. Rev. B **42**, 8752 (1990).
² T. R. Chien *et al.*, Phys. Rev. Lett. **67**, 2088 (1991).
³ Y. Zhao *et al.*, J. Phys. Condens. Matter **5** (22), 3623 (1993).
⁴ A. M. Finkel'stein *et al.*, Physica C **168**, 370 (1990).
⁵ H. Alloul *et al.*, Phys. Rev. Lett. **67**, 3140 (1991).
⁶ M. Z. Cieplak *et al.*, Phys. Rev. B **46**, 5536 (1992).
⁷ K. Ishida *et al.*, J. Phys. Soc. Jpn. **62**(8), 2803 (1993).
⁸ R. E. Walstedt *et al.*, Phys. Rev. B, **48**, 10646 (1993).
⁹ A. V. Mahajan *et al.*, Phys. Rev. Lett. **72**, 3100 (1994).
¹⁰ P. J. Hirschfeld *et al.*, Phys. Rev. B **37**, 83 (1988).
¹¹ A. J. Millis *et al.*, Phys. Rev. B **37**, 4975 (1988).
¹² T. Hotta, J. Phys. Soc. Jpn. **62**, 274 (1993).
¹³ L. S. Borkowski, P. J. Hirschfeld, Phys. Rev. B **49**, 15404 (1994).
¹⁴ R. Fehrenbacher, M. R. Norman, Phys. Rev. B **50**, 3445 (1994).
¹⁵ S. M. Quinlan, D. J. Scalapino, Phys. Rev. B **51**, 497 (1994).
¹⁶ P. J. Hirschfeld, W. O. Puttika, D. J. Scalapino, Phys. Rev. B **50**, 10250 (1994).
¹⁷ D. Poilblanc, D. J. Scalapino and W. Hanke, Phys. Rev. Lett. **72**, 884 (1994).
¹⁸ J. S. Langer, Phys. Rev. **120**, 714 (1960).
¹⁹ J. Callaway, *Quantum Theory of the Solid State*, (Academic Press, New York, 1974), Chap. 5.
²⁰ For the C_{4V} -lattice of the Hubbard model there exist in general five different representations. At the considered impurity site-types $\nu = 0, 1, 2$, only s -, p - and d -wave representations contribute. The p -wave is degenerated ($p_x = p_y$). Different site-types ν are distinguished by their distance from the origin.
²¹ D. Poilblanc, H. J. Schulz, T. Ziman, Phys. Rev. B **47**, 3268 (1993); P. Beran, D. Poilblanc and R. G. Laughlin, submitted to Nuclear Phys. B.
²² N. Bulut *et al.*, Phys. Rev. Lett. **62**, 2192 (1989).
²³ D. Poilblanc, D. J. Scalapino and W. Hanke, Phys. Rev. B **50**, 13020 (1994).
²⁴ R. Preuss, W. Hanke, W. von der Linden, Phys. Rev. Lett. **75**, 1344 (1995).
²⁵ T. Xiang, J. M. Wheatley, Phys. Rev. B **51**, 11721 (1995).

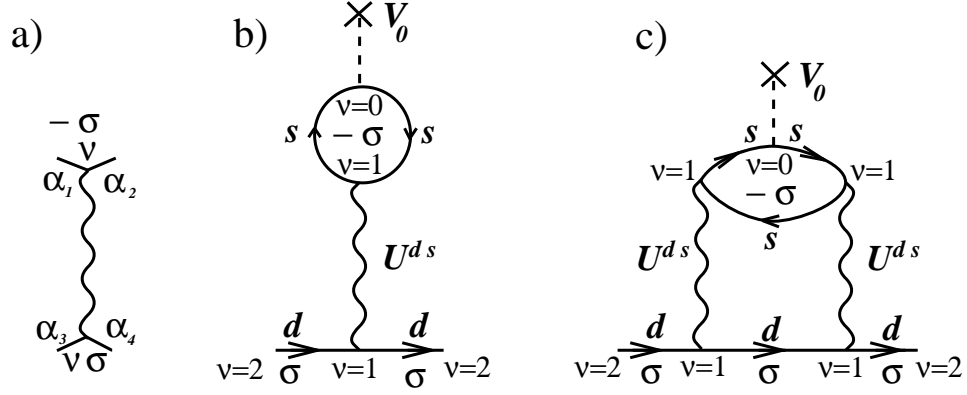


FIG. 1: Typical lowest order diagrams for the self-energy: a) Local interaction vertex connecting different symmetry channels. b),c) Diagrams of Σ_{UV} describing d -wave extended potential scattering of type 1; first order static contribution (b) and second order dynamic scattering process (c) in U . Scattering by the bare potential is depicted by a cross.

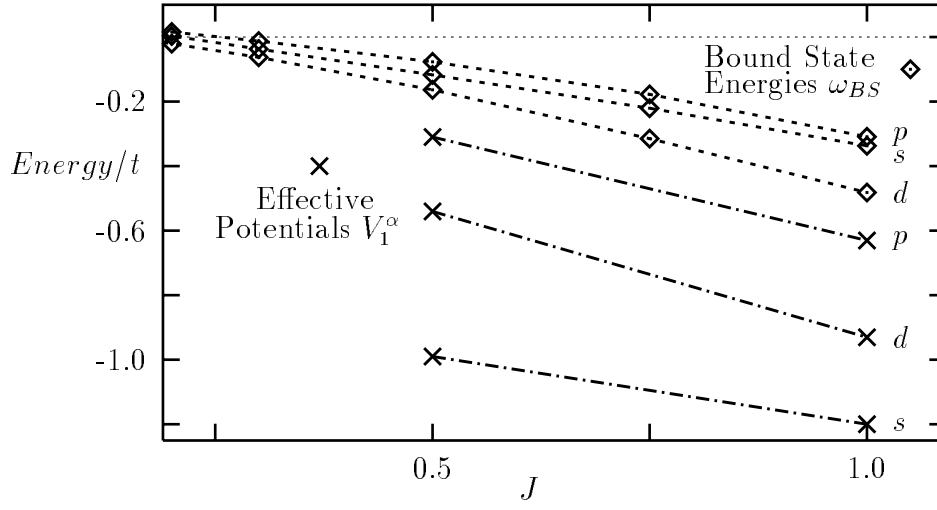


FIG. 2: Bound state energies ω_{BS} of an inert site in the t - J -model as a function of J [17]. The effective potentials V_1^α causing these states, derived by the generalized T-matrix method from a 26-site cluster.

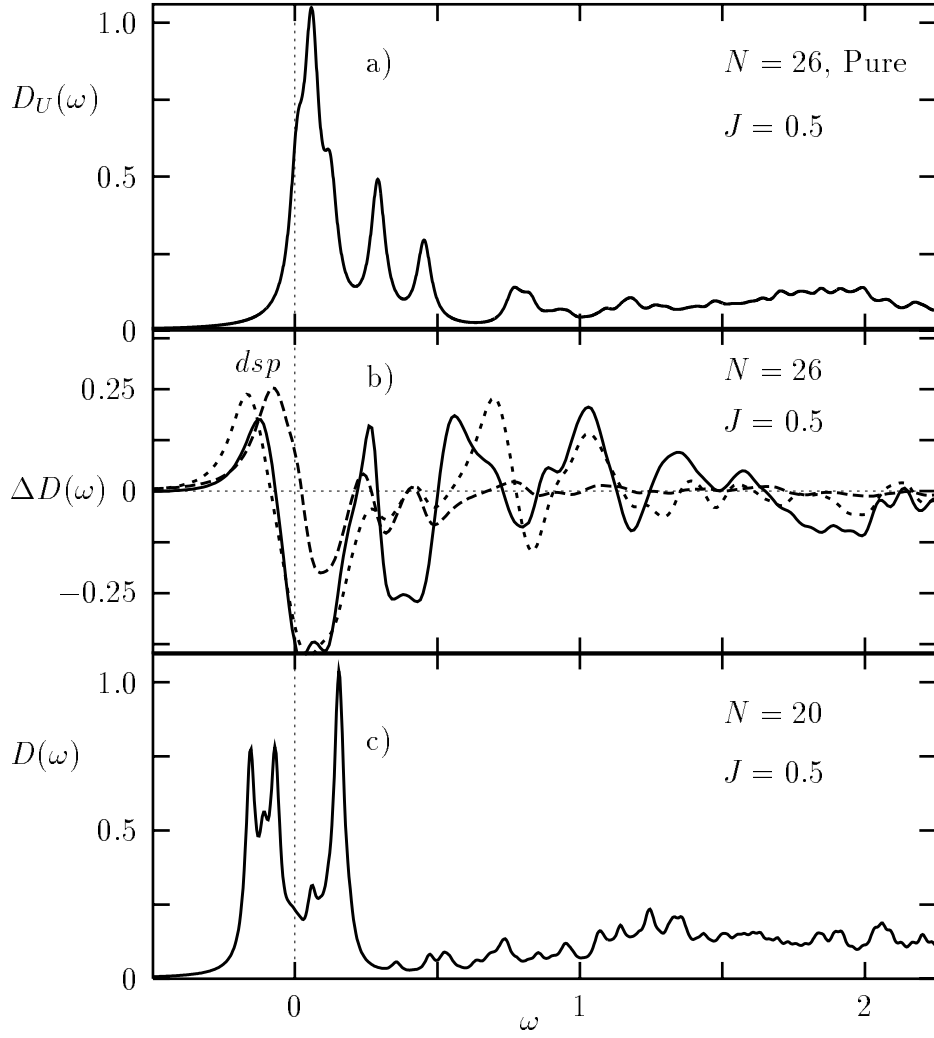


FIG3: a) Total density of states of the 26-site cluster without the impurity calculated exactly by ED. b) Additional density due to effective potentials at site types $\nu = 0, 1, 2$. d-wave: short-dashed lines, s-wave: solid lines, p-wave: long-dashed lines. c) Exact local density of states at site type $\nu = 1$ for a 20-site cluster with an inert site [17].

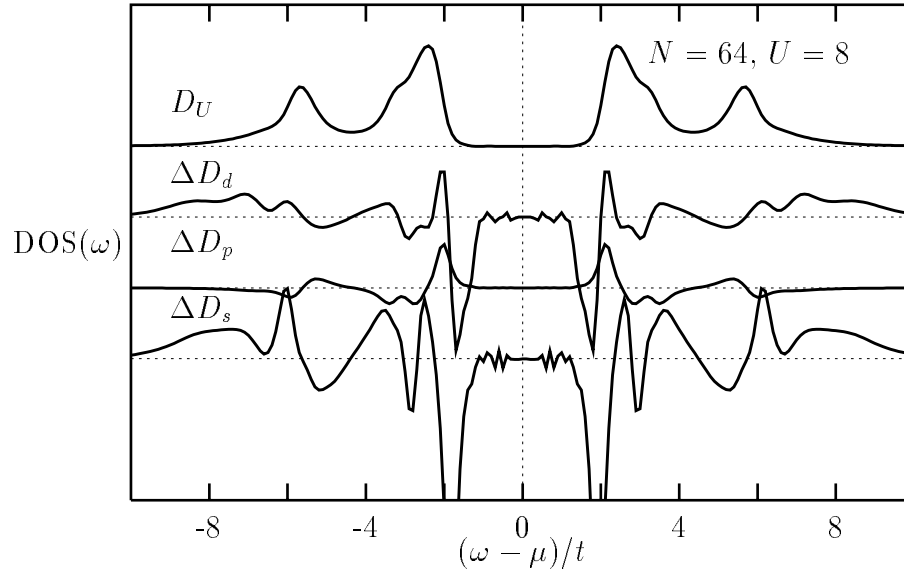


FIG. 4: Influence of effective potentials on the half-filled Hubbard model. D_U from QMC calculations ($\beta t = 10$). The appearance of various symmetry bound states causes gap-narrowing at the edges of the Hubbard bands.